Electronic Supplementary Information

Computational and solubility equilibrium experimental insight into Ca^{2+}-fluoride complexation and their dissociation behaviors in aqueous solutions: implication for the association constant measured using fluoride ion selective electrodes

Ning Zhang[a,*]; Jianfeng Tang[a]; Qiongqiong Luo[b]; Shaoheng Wang[b]; Dewen Zeng[b]

[a]*College of Science, Central South University of Forestry and Technology, Changsha 410004, Hunan, P.R. China*

[b]*College of Chemistry and Chemical Engineering, Central South University, Changsha 410083, Hunan, P.R. China*

[*]Corresponding author:

E-mail: ningcheung@hotmail.com

Tel: +86 13469075813

1. Technical details of CMD simulations

An extended simple point charge (SPC/E) model that has been used successfully for other brine systems [1-3] was employed for water molecules. Interactions between water molecules and the ions were defined by pairwise potentials. Long-range Coulombic interactions were handled by an Ewald summation [4] with a 12.0 Å cutoff; van der Waals interactions were modeled using the Lennard-Jones (LJ) potential. Cross terms for LJ interactions were derived from the Lorentz–Berthelot combination rules [5]. All parameters used in these simulations are listed in Table S1. These LJ potentials for Ca^{2+} and F^- have been used to model the Ca^{2+}-H_2O and F^--H_2O systems in previous studies [7,9].

All CMD simulations used a cubic box with periodic boundary conditions and the quaternion formulation of the rotational motion equations. Prior to canonical ensemble (NVT) runs, isothermal–isobaric ensemble (NPT) runs of 3 ns were carried out to determine an appropriate volume [10]. Pressure was maintained at 1 atm using the Nosé–Hoover barostat [11] with a 0.1 ps relaxation constant. Temperature was controlled by applying the Nosé–Hoover thermostat [11] with 0.5 ps relaxation times for NPT and NVT simulations. The Verlet velocity algorithm with a 1 fs time step was adopted, since this algorithm synchronizes the calculation of positions, velocities, and accelerations without sacrificing precision [12].

Table S1 Force field parameters for ions and water.

ion/water	σ (Å)	E (kcal·mol^{-1})	q (e)	Ref.
F^-	3.1180	0.1800	–1.000	[6]
Ca^{2+}	2.8721	0.1000	2.000	[7]
OW	0.1554	3.1655	–0.848	[8]
HW	-	-	0.424	[8]

2. Validity of force field parameters and convergence of simulations

2.1 Validity of force field parameters

The adoptive force field parameters for Ca^{2+} and F^- have been extensively used in previous studies [7,9,13,14] to explore the hydration behavior of Ca^{2+} and F^-. In present paper, we also applied them to explore the hydration behavior of Ca^{2+}, F^- and Ca-F CIPs and SSIPs. The results show that hydration number of Ca^{2+}/F^- and residence time of H_2O in their first hydration shell is 7.6/6.3 and 708/24.7 ps, respectively. These values are consistent with those (7.9/6.3 and 699/24.5 ps, respectively) reported from Koneshan et al.'s work [7]. Furthermore, the calculated diffusion constants for F^- and Ca^{2+} in the unbiased system are 1.06×10^{-5} and 0.46×10^{-5} cm^2·s^{-1}, respectively, which is also consistent with those of Koneshan et al.'s ($1.04 \pm 0.06 \times 10^{-5}$ and $0.53 \pm 0.03 \times 10^{-5}$ cm^2·s^{-1}). These indicate that our CMD runs are correct and their statistical equilibriums are achieved in current simulated time scale.

The hydration numbers for Ca^{2+} and F^- extracted from CMD simulations are somewhat higher than those optimized by DFT calculations which suggest that Ca^{2+} surrounded by 7 water molecules and F^- surrounded by 5 water molecules are more stable. However, for CaF_x^{2-x} (x = 1, 2), CMD and DFT consistently suggest that their seven-coordinated configurations are stable in aqueous solution.

Furthermore, the optimized Ca-F and Ca-O distances for the $CaF_x(H_2O)_y^{2-x}$ clusters are broad agreement with the results of CMD simulations, as shown in Table 2 (see text). Therefore, the force field parameters used in present text is credible.

2.2 Convergence of simulations

In present work, total running time for each CMD simulation is up to 14 ns including 3 ns NPT, 3 ns NVT and 8 ns NVT runs for determination of box size, pre-equilibrium and equilibrium, respectively. The obtained bond lengths of Ca-O and Ca-F are broad agreement with those of DFT calculations, as shown Table 2. Meanwhile, as stated above, the diffusion constants for F^- and Ca^{2+} also agree with those previously reported from Koneshan et al.'s [7] very well. And Koneshan et al.'s total running time (and their simulations with the force field are same as our) is less than 1 ns. This means that the 14 ns running for our CMD is enough to achieve equilibrium. Nevertheless, we still continue to run 4 ns for the unbiased system. The rear 3 ns trajectory data were collected to analyze. The RDFs of Ca-O and Ca-F pairs, along with those of Figs. 1a and 1b (see text) for comparison, are shown in Fig. S1. It could be seen that there is no significant change in all features of RDFs. This suggests again that the simulation times in text are enough to achieve convergence.

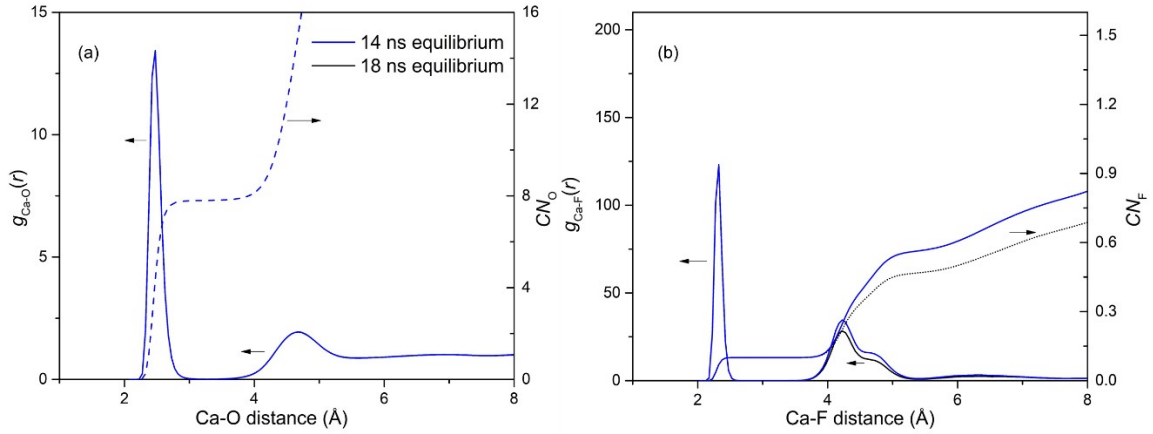

Fig. S1 RDFs of Ca-O (a) and Ca-F (b) and their integration extracted from the rear 3 ns data of CMD simulation with 18 ns equilibrium, along with those of 14 ns equilibrium for comparison.

For AIMD, we also continue to run 9 ps for the **AbMD-box-b4**. The total equilibrium time is up to 29 ps for this system. The distances of Ca-O and Ca-F as a function of run time are shown in Fig. S2. It could be seen that the H_2O and F^- bound with Ca^{2+} only slight oscillate at equilibrium position. The H_2O and F^- escaping from (or exchange in) the primary shell of Ca^{2+} is not observed, indicating that the seven-coordinated configuration is kept in overall running. We also sampling the snapshots of 8000 to 20000 and the snapshots of 25000 to simulation end and plot the RDFs of Ca-O and Ca-F pairs in Fig. S3. It could be seen that all features show no significant change in the RDFs for different sampling, suggesting that simulations have reached equilibrium.

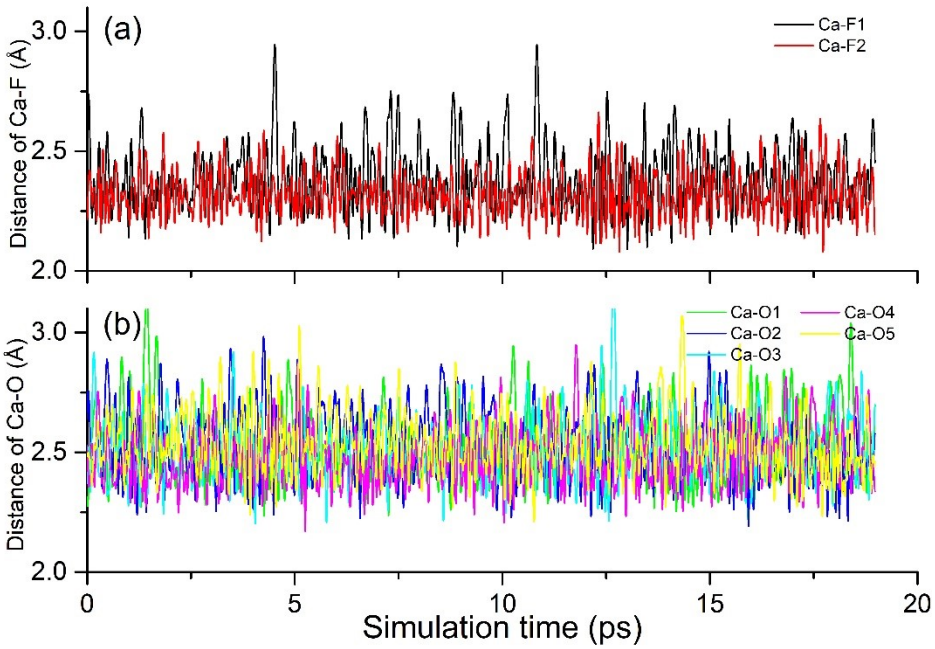

Fig. S2 Varying of distances of Ca-F (a) and Ca-O (b) as a function of simulation time. The pre-equilibrium times are not included.

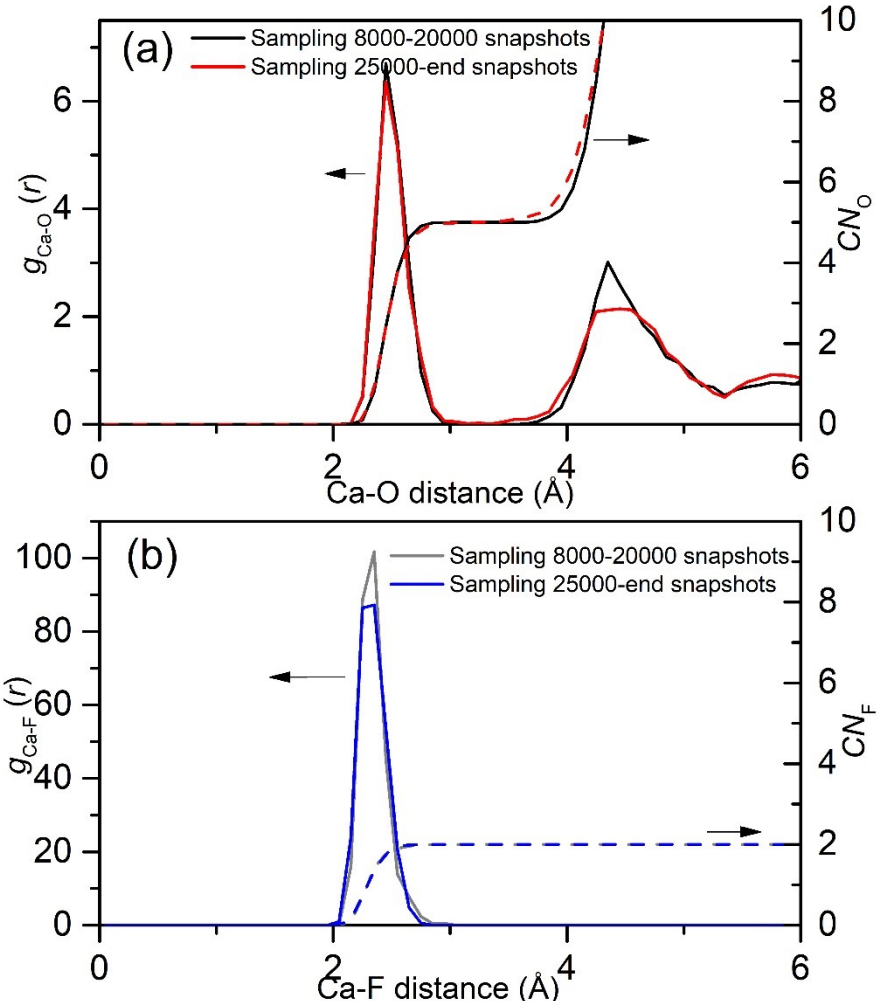

Fig. S3 RDFs of Ca-O (a) and Ca-F (b) and their integration extracted from 8000 to 20000 snapshots (black/gray) and 25000 to simulation end snapshots (red/blue), respectively.

3. Technical details of *ab initio* MD simulations

In the CP2K/QUICKSTEP package, the implementation of DFT based on a hybrid Gaussian and plane waves (GPW) basis sets scheme [15]. The Becke exchange and the Lee−Yang−Parr correlation functional (BLYP) [16,17] were utilized in addition to the dispersion correction (D2) put forth by Grimme [18] with a 40 Å cutoff. The dispersion corrections for the hydration structure of Ca^{2+} and energy barrier of Ca^{2+}-Cl^- pairing is very important, as reported in recent study [19]. For calculating the interactions between core and valence states, the auxiliary plane wave cutoffs of 400 Ry were used in conjunction with analytic Goedecker-Teter-Hutter (GTH) pseudopotentials [20,21] and a double-zeta valence polarized (DZVP) level basis set [22] generated using the valence electron configuration $1s^1$, $2s^2p^4$, $2s^2p^5$ and $3s^2p^64s^2$ for H, O, F and Ca, respectively.

All *ab initio* MD simulations were performed in the canonical ensemble (NVT) with the Nosé-Hoover chain thermostat [23] for ions and electrons at 300 K. In these simulations, a time step of 0.5 fs and the cubic box with a side length of 12.43 Å using periodic boundary conditions to eliminate interface effects were employed.

4. Details for the calculations of association constant for CaF_x^{2-x}

As our simulations were performed at a constant cell volume, the energy of equation (S1) is a $\Delta_r A$ rather than a $\Delta_r G$. However, the energy difference of $\Delta_r A$ and $\Delta_r G$ for the ligand exchange reaction is in the order of 0.01-0.1 kJ·mol^{-1} (i.e., ≤ 0.01 log unit) [24]; thus, the difference between $\Delta_r A$ and $\Delta_r G$ was ignored in subsequent association constant calculations. This assumption has been adopted in previous studies [25-27].

The $\Delta_r G^\Theta$ for equation (2) (see text) can be obtained by concentration and activity corrections for $\Delta_r G$, according to

$$\Delta_r G^\Theta = \Delta_r G + RT\ln\frac{C_A\gamma_A \cdot C_B\gamma_B}{C_C\gamma_C \cdot C_D\gamma_D} \quad \text{(S1)}$$

where c_i are the concentrations of reactants or products for the reaction A + B → C + D and γ_i are the corresponding activity coefficients which were estimated by the b-dot extension [28]:

$$\log\gamma_i = -\frac{z_i^2 A_\gamma I^{0.5}}{1 + \dot{a}_i B_\gamma I^{0.5}} + \dot{B}_\gamma I \quad \text{(S2)}$$

where z_i is the charge of the individual ion i, I is the ionic strength, A_γ and B_γ are constants with the values of 0.5092 kg$^{0.5}$·mol$^{-0.5}$ and 0.3283 kg$^{0.5}$·mol$^{-0.5}$·Å^{-1}, respectively [28], $\dot{B}_\gamma$ is an empirical parameter with the values of 0.038 kg·mol^{-1} [29], $\dot{a}_i$ is the ion size parameter in Å ($\dot{a}_i$ = 3.5, 6.0 and 5.0 for F^-, Ca^{2+} and CaF_x^{2-x} complexes, respectively) [30]. Finally, the $\log K^\Theta$ were calculated by:

$$\Delta_r G^\Theta = -2.303RT\log K^\Theta \quad \text{(S3)}$$

There are a number of sources for errors in our $\log K^\Theta$ calculations using the *ab initio* thermodynamic integration as described above. First, the activity coefficient of individual ion estimated by equation (S2) to correct the $\Delta_r G$ to the standard state of infinite dilution can introduce

some error due mainly to the lack of $\dot{a}_i$ for CaF_x^{2-x} complexes. In previous work Liu et al. have shown that the effects of uncertainty for $\dot{a}_i$ give a change of less than 0.05 log unit for $\Delta\dot{a}_i = \pm 1$ on the derived $\log K^{\Theta}$ values for $CuCl_x^{1-x}$ (x = 1, 2, 3) complexes [31]. Second, the size of simulation box used might have some effect. In current work, we have used a simulation box large enough to include the first solvation shell of the Ca^{2+}, F^- and their complexes. Recently, Guan et al. has shown that this effect generates a difference of < 0.3 log unit between both cubic boxes with side length of ~12 Å (containing 55 H_2O) and ~17 Å (110 H_2O) for YCl_x^{3-x} (x = 1, 2) complexes [27]. Finally, there is also an error due to the systematic and statistical imprecision caused by the sampling averages over runs of finite length. This uncertainty can be estimated by calculating the statistical error of $\langle f(r) \rangle$ with a statistical inefficiency value, as described in previous study [5]. This approach has been adopted by some authors [32,33].

5. Details of DFT calculations

All optimizations were carried out by static DFT calculations using Becke's three-parameter exchange potential and Lee-Yang-Parr correlation functional (B3LYP) [16,17,34] with the Grimme's D3 correction [35] in the Gaussian 09 software package [36]. A Stuttgart relativistic effective core potential (RECPs) [37] were employed in conjunction with the basis set to describe the valence electrons of Ca. For F, O and H, Dunning's correlation-consistent basis sets, aug-cc-pVDZ [38], were used.

6. Details of solubility equilibrium experiment

Separate binary stock solutions of KCl and KF were prepared and their concentrations were determined by precipitation method with sodium tetraphenylborate as precipitating agent [39]. A series of mixed KCl + KF solutions, with varied concentration but their total ionic strength remained at constant ~4 mol·kg^{-1}, were prepared gravimetrically by mixing the binary stock solutions. The composition of these solutions was summarized in Table S2.

About 2 g CaF_2 powder was added into each mixed KCl + KF solution as equilibration solid. Then, they were immersed in the waterbath thermostat with constant temperature at 25.00 ℃. The waterbath temperature of thermostat was controlled by a Lauda E200 heater combining a Lauda DLK25 through-flow cooler (Germany) with uncertainty of ±0.05 ℃. To enhance the dissolution kinetics of $CaF_{2(s)}$, the magnetic rotor, driven by the magnetic stirrer below the flasks, was placed in each flask to stir the solution and solid phase. The equilibrium time of all samples was reached 30 days, which is enough for the dissolution equilibrium of $CaF_{2(s)}$ in these solutions [40].

After reaching equilibrium, the magnetic stirrer was turned off and all samples were silently placed in the waterbath for 2 days at 25.00 ℃. Subsequently, the supernate in each flask was extracted *via* the microfiltration member with the aperture of 0.45 μm, preventing the undissolved fine particle of $CaF_{2(s)}$, as the pre-analyzed samples. The Ca^{2+} concentration was analyzed by ICP-OES (Thermo Scientific iCAP 7200 Radial, Thermo Fisher Scientific, USA) with the standard curve

method [41].

The equilibrium and analyzed methods described above have been successfully applied to determine the solubility data of MF_2 (M = Ca, Mg, Zn, Mn) in different mixed (binary and ternary) electrolytes with varied temperature in our laboratory [40,42,43].

Table S2 Solution compositions for $CaF_{2(s)}$ dissolution equilibrium experiment at 298.15 K

Serial number	KF (mol·kg^{-1})	KCl (mol·kg^{-1})	Ion strength (mol·kg^{-1})
1	0.00568	3.9916	3.99728
2	0.00975	3.9909	4.00065
3	0.05017	3.9369	3.98707
4	0.09949	3.9003	3.99979
5	0.50104	3.4997	4.00074
6	0.99881	3.0005	3.99931
7	1.99929	2.0010	4.00029
8	3.00067	0.9998	4.00047

7. Exchange of F^- in primary shell of Ca^{2+}

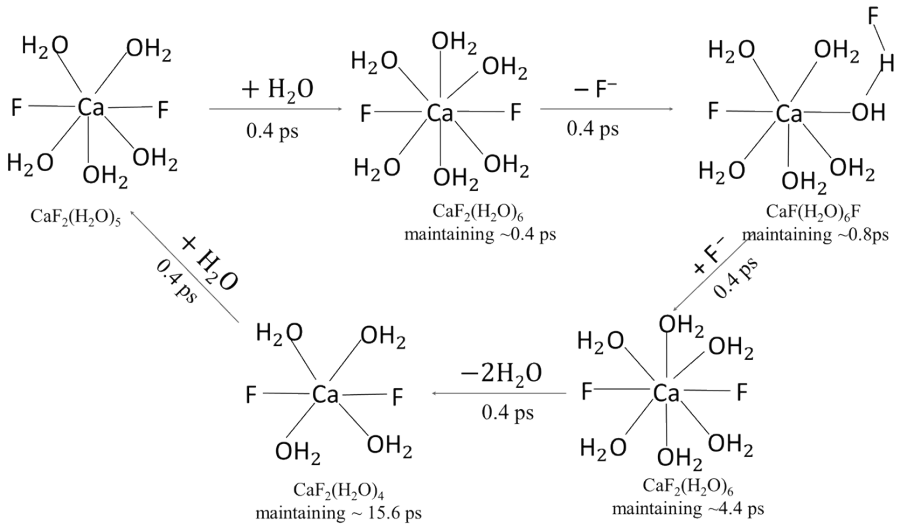

Fig. S4 Schematic representation of the exchange process of F^- in primary shell of Ca^{2+}.

8. Additional DFT information

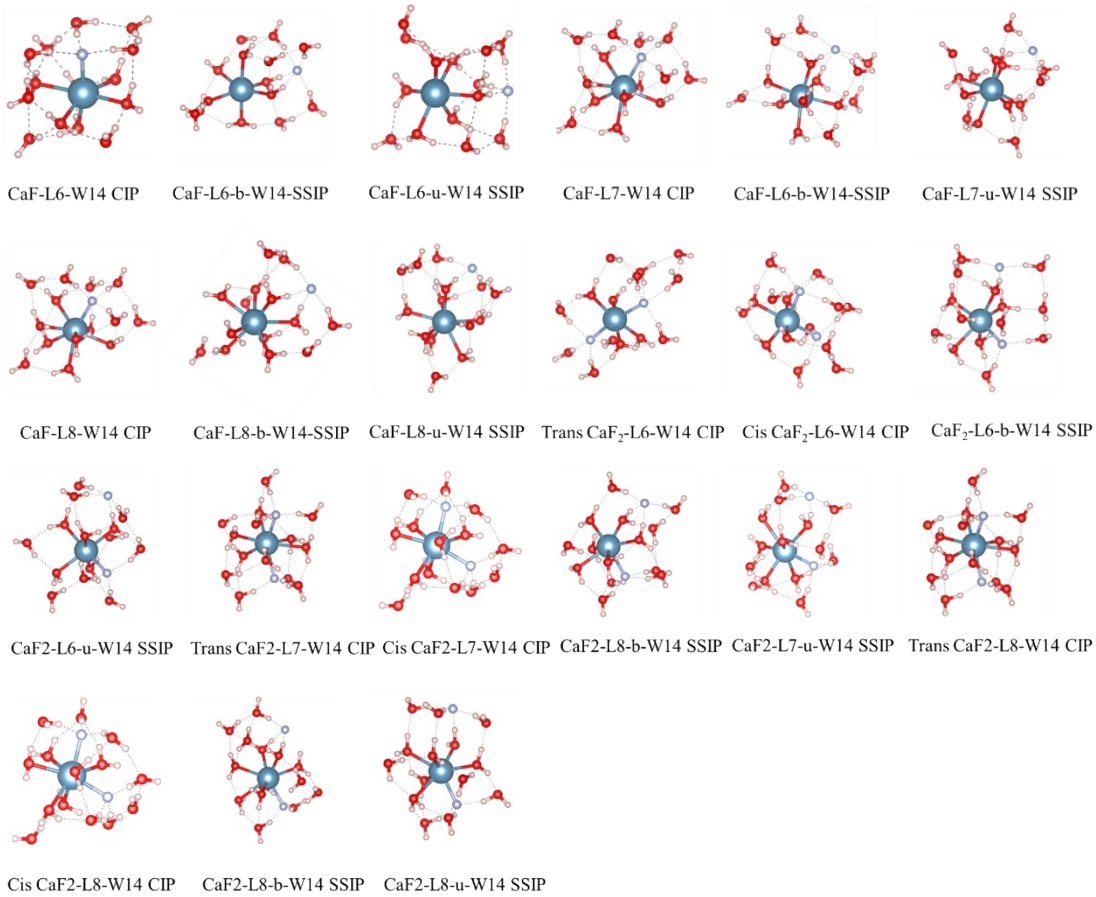

Fig. S5 Selected optimized structures of $CaF_x(H_2O)_{14}^{2-x}$ (x = 1, 2) CIP and SSIP clusters. Other optimized structures that are quite less stable were not shown. The hydrogen bonds formed among water molecules are displayed by the dashed lines. Color code: Cyan, Ca; gray, F; red, O; pink, H.

9. RDF of Ca-F pair for the unbiased simulations with normal/ fictitious Ca/F charge

To further clarify strong electrostatic interactions on the formation of Ca^{2+}-F^- CIPs and SSIPs, we applied a fictitious scaling factor 0.7 to the normal charge of Ca/F to weaken the electrostatic interactions in the unbiased simulations where all parameters is same as the original one apart from the charges of Ca^{2+} and F^- with +1.4 and −0.7, respectively. The RDF of Ca-F pair for system with scaling charge, along with that with normal charge for comparison, is shown in Fig. S6. Compared to the latter, the first and second peaks, representing the Ca-F CIPs and SSIPs, respectively, show a right shift and a reduced intensity of both peaks for former, suggesting that interaction of Ca^{2+} and F^- weaken. This supports that the formation of Ca^{2+}-F^- CIPs and SSIPs is govern by strong electrostatic interaction.

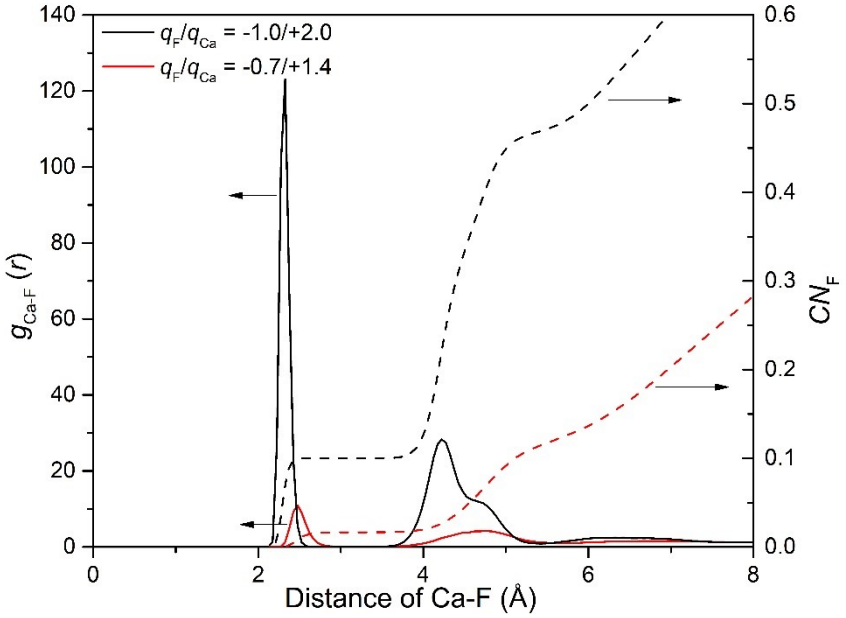

Fig. S6 RDFs for Ca-F pair (solid lines), as well as the corresponding integrals (dashed lines) for **CMD-box-u** with q_F/q_{Ca} of −1.0/+2.0 (black) and −0.7/+1.4 (red), respectively.

References

1. L. Fulton, M. Hoffmann, J.G. Darab, B.H. Palmer. Copper(I) and copper(II) coordination structure under hydrothermal conditions at 325 °C: An X-ray absorption fine structure and molecular dynamics study. J. Phys. Chem. A 2000, 104: 11651-11663.
2. H.J. Li, H.B. Yi, J.J. Xu. High-order Cu(II) chloro-complexes in LiCl brines: Insights from density function theory and molecular dynamics. Geochim. Cosmochim. Acta 2015, 165: 1-13.
3. N. Zhang, J. Tang, Y. Ma, M. Liang, D. Zeng, G. Hefter. A spectroscopic study of solvent effects on formation of Cu(II)-chloride complexes in aqueous solution. Phys. Chem. Chem. Phys. 2021, 23: 6807-6814.
4. U. Essmann, L. Perera, M.L. Berkowitz, T. Darden, H. Lee, L.G. Pedersen. A smooth particle mesh Ewald method. J. Chem. Phys. 1995, 103: 8577-8593.
5. M.P. Allen, D.J. Tildesley. Computer simulation of liquids. Oxford University Press, 1987.
6. L.X. Dang. Fluoride-fluoride association in water from molecular dynamics simulations. Chem Phys Lett. 1992, 200: 21-25.
7. S. Koneshan, J.C. Rasaiah, R. M. Lynden-Bell, S. H. Lee. Solvent structure, dynamics, and ion mobility in aqueous solutions at 25 °C. J. Phys. Chem. B. 1998, 102: 4193-4204.
8. H.J. Berendsen, J.R. Grigera, T.P. Straatsma. The missing term in effective pair potentials. J. Phys. Chem. 1987, 91: 6269-6271.
9. H.S. Lee. Molecular dynamics simulation study for ion mobility of alkali earth metal cations in water at 25 °C. Mol. Simulat. 2013, 39: 895-901.
10. D.L. Pincus, C. Hyeon, D. Thirumalai. Effects of trimethylamine N-oxide (TMAO) and crowding agents on the stability of RNA hairpins. J. Am. Chem. Soc. 2008, 130: 7364-7372.
11. W.G. Hoover. Canonical dynamics: equilibrium phase-space distributions. Phys. Rev. A 1985, 31: 1695-1697.
12. S.A. Adcock, J.A. Mccammon. Molecular dynamics: survey of methods for simulating the activity of proteins. Chem. Rev. 2006, 106: 1589-1615.
13. S.H. Lee, C. Jayendran. Molecular dynamics simulation of ion mobility. 2. Alkali metal and halide ions using the SPC/E model for water at 25 °C. J. Phys. Chem. 1996, 100: 1420-1425.
14. Y. Wang, Y. Li, H. Yi. High-order Ca(II)-chloro complexes in mixed $CaCl_2$-LiCl aqueous solution: Insight from density functional theory and molecular dynamics simulations. J. Phys. Chem. 2016, 120: 5635-5648.
15. G. Lippert, J. Hutter, M. Parrinello. A hybrid gaussian and plane wave density functional

scheme. Mol. Phys. 2010, 92: 477-487.
16. A.D. Becke. Density-functional exchange-energy approximation with correct asymptotic behavior. Phys. Rev. A 1988, 38: 3098-3100.
17. C. Lee, W. Yang, R.G. Parr. Development of the colle-salvetti correlation-energy formula into a functional of the electron density. Phys. Rev. B 1988, 37: 785-789.
18. S. Grimme. Accurate description of van der waals complexes by density functional theory including empirical corrections. J. Comput. Chem. 2004, 25: 1463-1473.
19. M.D. Baer, C.J. Mundy. Local aqueous solvation structure around Ca^{2+} during Ca^{2+}…Cl^{-} pair Formation. J. Phys. Chem. B 2016, 120: 1885-1893.
20. S. Goedecker, M. Teter, J. Hutter. Separable dual-space gaussian pseudopotentials. Phys. Rev. B 1996, 54, 1703-1710.
21. C. Hartwigsen, S. Goedecker, J. Hutter. Relativistic separable dual-space gaussian pseudopotentials from H to Rn. Phys. Rev. B 1998, 58: 3641-3662.
22. J. VandeVondele, J. Hutter. Gaussian basis sets for accurate calculations on molecular systems in gas and condensed phases. J. Chem. Phys. 2007, 127: 114105.
23. S. Nosé. A unified formulation of the constant temperature molecular dynamics methods. J. Chem. Phys. 1984, 81: 511-519.
24. Y. Mei, D.M. Sherman, W. Liu, J. Brugger. Ab initio molecular dynamics simulation and free energy exploration of copper(I) complexation by chloride and bisulfide in hydrothermal fluids. Geochim. Cosmochim. Acta. 2013, 102: 45-64.
25. N. Zhang, E. Königsberger, S.Q. Duan, K. Lin, H.B. Yi, D.W. Zeng, Z.W. Zhao, G. Hefter. Nature of monomeric molybdenum(VI) cations in acid solutions using theoretical calculations and Raman spectroscopy. J. Phys. Chem. B 2019, 123: 3304-3311.
26. N. Zhang, H.B. Yi, D.W. Zeng, Z.W. Zhao, W.L. Wang, F. Costanzo. Structure evolution of mononuclear tungsten and molybdenum species in the protonation process: Insight from FPMD and DFT calculations. Chem. Phys. 2018, 502: 77-86.
27. Q. Guan, Y. Mei, B. Etschmann, D. Testemale, M. Louvel, J. Brugger. Yttrium complexation and hydration in chloride-rich hydrothermal fluids: A combined ab initio molecular dynamics and in situ X-ray absorption spectroscopy study. Geochim. Cosmochim. Acta. 2020, 281: 168-189.
28. H.C. Helgeson, D.H. Kirkham. Theoretical prediction of the thermodynamic behavior of aqueous electrolytes at high pressures and temperatures: II. Debye-Hückel parameters for activity coefficents and relative partial molal properties. Am. J. Sci. 1974, 274: 1199-1261.
29. H.C. Helgeson, D.H. Kirkham, G.C. Flowers. Theoretical prediction of the thermodynamic behavior of aqueous electrolytes at high pressures and temperatures: IV. Calculation of activity coefficients, osmotic coefficients, and apparent molal and standard and relative partial molal properties to 600 ℃ and 5 Kb. Am. J. Sci. 1981, 281: 1249-1516.
30. J. Kielland. Individual activity coefficients of ions in aqueous solutions. J. Am. Chem. Soc. 1937, 59: 1675-1678.
31. W. Liu, J. Brugger, D.C. Mcphail, L. Spiccia. A spectrophotometric study of aqueous copper(I)-chloride complexes in LiCl solutions between 100 ℃ and 250 ℃. Geochim. Cosmochim. Acta. 2002, 66: 3615-3633.
32. T. Rodinger, P.L. Howell, R. Pomès. Absolute free energy calculations by thermodynamic integration in four spatial dimensions. J. Chem. Phys. 2005, 123: 034104.
33. Y. Mei, W. Liu, J. Brugger, D.M. Sherman, J.D. Gale. The dissociation mechanism and thermodynamic properties of $HCl_{(aq)}$ in hydrothermal fluids (to 700 ℃, 60 kbar) by ab initio molecular dynamics simulations. Geochim. Cosmochim. Acta. 2018, 226: 84-106.
34. J.P. Perdew. Density-functional approximation for the correlation energy of the inhomogeneous electron gas. Phys. Rev. B 1986, 33: 8822-8824.
35. S. Grimme, J. Antony, S. Ehrlich, J. Krieg. A consistent and accurate ab initio parametrization of density functional dispersion correction (DFT-D) for the 94 elements H-Pu. J. Chem. Phys. 2010, 132: 154104.
36. M.J. Frisch, G.W. Trucks, H.B. Schlegel, G.E. Scuseria, M.A. Robb, J.R. Cheeseman, G. Scalmani, V. Barone, B. Mennucci, G.A Petersson, et al. Gaussian 09, Revision E.01; Gaussian, Inc.: Wallingford, CT, 2009.
37. M. Kaupp, P.V.R. Schleyer, H. Stoll, H. Preuss. Pseudopotential approaches to Ca, Sr, and Ba hydrides. Why are some alkaline earth MX2compounds bent? J. Chem. Phys. 1991, 94: 1360-

1366.
38. T.H.J. Dunning. Gaussian basis sets for use in correlated molecular calculations. I. The atoms boron through neon and hydrogen. J. Chem. Phys. 1989, 90: 1007-1023.
39. B. Fan, D. Chu, Z. Shang. Improvement on determination of water-soluble potassium content in fertilizers by potassium tetraphenylborate gravimetric method and development of related international standard. Sci. Technol. Rev. 2014, 32: 32-38.
40. S.H. Wang, Q.Q. Luo, N. Zhang, D.W. Zeng. Solubility measurement of the systems MF_2 (M = Ca, Mg, Zn) + $ZnSO_4$ + H_2O and MF_2 (M = Ca, Mg) + ZnF_2 + H_2O at 298.15 K. J. Chem. Eng. Data 2019, 64: 3078-3084.
41. Analytical Laboratory of Qinghai Institute of Salt Lakes at Chinese Academy of Sciences. Analytic Method of Brines and Salts. Beijing: Science Press, 1988.
42. Q.Q. Luo, S.H. Wang, D.W. Zeng, Y.N. Wang. Solubility Phase Equilibrium of the Quaternary Reciprocal System Ca^{2+}, Mn^{2+}//F^{-}, SO_4^{2-} + H_2O at 298.15 K. J. Chem. Eng. Data 2019, 64: 1834-1839.
43. H.L. Li, S.H. Wang, D.W. Zeng. Experimental measurement of the solid–liquid equilibrium of the systems MF_2 + H_2O (M = Mg, Ca, Zn) from 298.15 to 353.15 K. J. Chem. Eng. Data 2018, 63: 1733-1736.